Published in final edited form as:
J Am Chem Soc. 2009 April 22; 131(15): 5388–5389. doi:10.1021/ja901658c.

A Direct Route to Cyclic Organic Nanostructures via Ring-Expansion Metathesis Polymerization of a Dendronized Macromonomer

Andrew J. Boydston[a], **Thomas W. Holcombe**[b], **David A. Unruh**[b], **Jean M. J. Fréchet**[b,*], and **Robert H. Grubbs**[a,*]

[a]Arnold and Mabel Beckman Laboratory of Chemical Synthesis, Division of Chemistry and Chemical Engineering, California Institute of Technology, Pasadena, CA 91125

[b]College of Chemistry, University of California, Berkeley, CA 94720

Controlling polymer topology presents challenging synthetic obstacles as well as exciting opportunities for tuning macromolecular properties.[1] In particular, nanoscale molecular architectures with well-defined shapes and dimensions may provide significant advancements in areas such as drug delivery and nanotechnology. Over the last decade, breakthroughs in polymer syntheses have greatly increased the variety of macromolecular architectures that may be obtained, including dendronized, cylindrical, star, hyperbranched, and cyclic polymers as well as various block copolymers.[2,3] However, the synthesis of circular nanostructures remains challenging due in large part to the difficulty in preparing functionalized cyclic polymers.[4] Furthermore, reliance on macrocyclization routes to cyclic polymers restricts attachment of large side chains or dendrons to post-polymerization, and an efficient route to cyclic hybrid architectures of high purity is yet to be realized. Following recent developments in ring-expansion metathesis polymerization (REMP)[5] and linear dendronized polymers,[6] we aimed to interface these two areas to achieve a direct, efficient route to cyclic organic nanostructures.[7] Herein, we report the REMP of a dendronized macromonomer (MM) as well as confirmation of cyclic polymer topology via atomic force microscopy (AFM).

REMP utilizes Ru-based metathesis catalysts (Figure 1) capable of producing cyclic polymers directly from cyclic olefin monomers, thus avoiding linear polymeric synthons. Earlier studies revealed that N-heterocyclic carbene backbone saturation greatly increased overall catalyst activity, while tether length influenced the relative rates of propagation vs catalyst release. With access to a range of catalyst activities, we envisioned that REMP of dendronized MMs may achieve dendronized cyclic polymers in a single operation. In addition, REMP can produce high molecular weight (MW) cyclic polymers, a goal not easily accomplished using macrocyclization processes.

While the polymerization of sterically hindered MMs presents an inherent challenge, it was shown that **1** (Figure 1) could be efficiently polymerized via ROMP using a highly active Ru-based metathesis catalyst. This approach to dendritic polymers is particularly attractive, in that post-polymerization modifications are unnecessary, ensuring that complete dendron functionality is present along the polymer backbone.[2c] Thus, we examined the efficiency of REMP using **1** in combination with cyclic catalysts **SC-5** and **UC-6**.

rhg@caltech.edu and frechet@berkeley.edu.

Supporting Information Available Detailed experimental procedures and AFM images of $\mathbf{P1_{son}}$. This materials is available free of charge *via* the Internet at http://pubs.acs.org

Saturated catalyst **SC-5** was found to mediate REMP of **1** and key data are summarized in Table 1. In general, polymerizations required higher temperatures (55 °C) and higher loadings of $[\mathbf{1}]_0/[\mathbf{SC\text{-}5}]_0$ than used in previous studies involving cyclooctene monomers, which is ascribed to the steric bulk of MM **1**. Interestingly, an inverse relationship between reaction concentration and degree of polymerization (DP) of polymer **P1** was observed. Specifically, REMP of **1** ($[\mathbf{1}]_0/[\mathbf{SC\text{-}5}]_0$ = 50:1) at $[\mathbf{1}]_0$ = 0.05, 0.10, 0.20, and 0.33 M resulted in polymers having DPs of 5840, 4510, 4330, and 2190, respectively (entries 1, 2, 5, and 6). Since each polymerization reached full monomer conversion, this trend suggests that the initiation rate increases more with increased reaction concentration than does the propagation rate. Additionally, because incomplete initiation is observed with catalyst **SC-5**, the increased reaction concentration essentially led to a greater number of growing polymer rings and therefore a lower average MW.

Increasing the $[\mathbf{1}]_0/[\mathbf{SC\text{-}5}]_0$ resulted in incomplete monomer conversion due to catalyst death over the extended reaction periods. However, as expected, increased $[\mathbf{1}]_0/[\mathbf{SC\text{-}5}]_0$ ratios resulted in higher M_w values. Specifically, using $[\mathbf{1}]_0/[\mathbf{SC\text{-}5}]_0$ = 100:1 polymer **P1** with M_w = 4.47 MDa (entry 3) was obtained, whereas M_w = 5.33 MDa was obtained with $[\mathbf{1}]_0/[\mathbf{SC\text{-}5}]_0$ (entry 4). Notably, catalyst **UC-6** efficiently polymerized **1** to >95% conversion at $[\mathbf{1}1]_0/[\mathbf{UC\text{-}6}]_0$ = 250:1. These conditions provided **P1** with a M_w = 3.79 MDa (entry 7).

Catalyst release and reincorporation have been shown to guide the thermodynamically driven MW of REMP polymers. In the present case, catalyst reincorporation and chain transfer are unlikely considering the steric bulk of MM **1**. Notably, the MW of **P1** did not change upon prolonged standing after 100% monomer conversion, or upon injection of fresh catalyst into the reaction mixtures. This indicates that thermodynamic equilibration of ring sizes is not taking place. Furthermore, the MW of isolated **P1** did not increase upon treatment with additional **1**, suggesting that no significant amount of active Ru species remain in the cyclic polymer. Collectively the data suggests efficient, irreversible catalyst release, and an absence of chain transfer events. These experiments provide an initial investigation into the kinetically controlled MW profile of REMP.

We next turned our attention toward visualization of the polymers via AFM.[8] Samples of **P1** were prepared by spin-coating a 9 ng/mL solution of the polymer in $CHCl_3$ onto freshly cleaved mica. As shown in Figure 2, toroidal features were observed with diameters of ca 35 - 40 nm, heights ranging from 5 - 9 Å, and internal diameters ranging from ca 5 - 7 nm. Multiple rings were observed (Figure 2A) without any detectable linear polymers, and analysis of the line scans of the toroids revealed highly uniform profile features (Figure 2D). Considering the high DP values obtained for **P1**, the dimensions observed via AFM suggested that the polymer backbone is not fully extended and may be adopting a zigzag orientation.

For comparison, we also examined linear analogues via AFM. Because the high DPs obtained via REMP were difficult to achieve using acyclic ROMP catalysts, we investigated ring-opening of **P1** via sonication. Given that polymer chain scission can be induced via ultrasound,[9] and that the steric congestion may weaken the backbone of **P1**, we subjected a solution of cyclic polymer (M_w = 2.99 MDa, 1 mg/mL in THF) to ultrasound irradiation for 30 min to give $\mathbf{P1_{son}}$. GPC analysis of $\mathbf{P1_{son}}$ revealed an M_w = 959 kDa, which suggests that chain scission accompanied ring-opening. In addition, $\mathbf{P1_{son}}$ displayed shorter elution times at the same MW in comparison with **P1**, consistent with linear and cyclic topologies, respectively (Figure 3).[10] AFM imaging of $\mathbf{P1_{son}}$ revealed features consistent with a linear topology (see the Supporting Information). Notably, some features resembled those of the cyclic polymers in diameter and shape; however these did not appear toroidal as no central void was observed. This may be ascribed to aggregation, which is more commonly observed upon AFM imaging of the linear polymers in comparison with cyclic **P1**.

In conclusion, we have demonstrated the first direct synthesis of cyclic dendronized polymers via REMP of a dendronized macromonomer. AFM imaging has confirmed the cyclic topology, revealing uniform cyclic features with no detectable linear polymer contaminants. The kinetically controlled molecular weight profiles and relative initiation versus propagation rates of REMP resulted in polymer M_w values that increased with decreasing initial concentrations. Despite the steric challenges inherent to the polymerization of these dendronized monomers, very high molecular weights were achieved for this novel class of hybrid macromolecules.

Supplementary Material

Refer to Web version on PubMed Central for supplementary material.

Acknowledgment

Financial support of this research by the National Science Foundation (CHE-0410425 and DMR-0906638) and the Department of Energy (DE-FG02-05ER46218). AJB thanks the National Institutes of Health for a postdoctoral fellowship. TWH thanks the National Science Foundation for a Graduate Research Fellowship.

References

1). (a) Nasongkla N, Chen B, Macaraeg N, Fox ME, Fréchet JMJ, Szoka FC. J. Am. Chem. Soc. in press (DOI: 10.1021/ja900062u) (b) Eugene DM, Grayson SM. Macromolecules 2008;41:5082–5084. (c) Guan Z. J. Polym. Sci., Part A: Polym. Chem 2003;41:3680–3692. (d) Guan Z. Chem. Eur. J 2002;8:3086–3092. (e) Harth EM, Hecht S, Helms B, Malmstrom EE, Fréchet JMJ, Hawker CJ. J. Am. Chem. Soc 2002;124:3926–3938. [PubMed: 11942830] (f) Edgecombe BD, Stein JA, Fréchet JMJ, Xu Z, Kramer EJ. Macromolecules 1998;31:1292–1304.

2). For reviews, see: (a) Matyjaszewski K, Xia J. Chem. Rev 2001;101:2921–2990. [PubMed: 11749397]. (b) Kamigaito M, Ando T, Sawamoto M. Chem. Rev 2001;101:3689–3746. [PubMed: 11740919]. (c) Schlüter AD, Rabe JP. Angew. Chem. Int. Ed 2000;39:864–883..

3). (a) Tezuka Y, Fujiyama K. J. Am. Chem. Soc 2008;127:6266–6270. [PubMed: 15853332] (b) Jeong W, Hedrick JL, Waymouth RM. J. Am. Chem. Soc 2007;129:8414–8415. [PubMed: 17579414] (c) Culkin DA, Jeong W, Csihony S, Gomez ED, Balsara NP, Hedrick JL, Waymouth RM. Angew. Chem. Int. Ed 2007;46:2627–2630. (d) Pyun J, Kowalewski T, Matyjaszewski K. Macromol. Rapid Commun 2003;24:1043–1059. (e) Bosman AW, Vestberg R, Heumann A, Fréchet JMJ, Hawker CJ. J. Am. Chem. Soc 2003;125:715–728. [PubMed: 12526671] (f) Shu L, Schlüter AD, Ecker C, Severin N, Rabe JP. Angew. Chem. Int. Ed 2001;40:4666–4669.

4). Schappacher M, Deffieux A. J. Am. Chem. Soc 2008;130:14684–14689. [PubMed: 18841891]

5). (a) Boydston AJ, Xia Y, Kornfield JA, Gorodetskaya IA, Grubbs RH. J. Am. Chem. Soc 2008;130:12775–12782. [PubMed: 18729450] (b) Xia Y, Boydston AJ, Gorodetskaya IA, Kornfield JA, Grubbs RH. J. Am. Chem. Soc 2009;131:2670–2677. [PubMed: 19199611]

6). Rajaram S, Choi T-L, Rolandi M, Fréchet JMJ. J. Am. Chem. Soc 2007;129:9619–9621. [PubMed: 17636929]

7). Laurent BA, Grayson SM. Polym. Prepr. (Am. Chem. Soc., Div. Polym. Chem.) 2008;49:287–288.

8). Sheiko SS, Möller M. Chem. Rev 2001;101:4099–4124. [PubMed: 11740928]

9). Mason, TJ.; Lorimer, JP., editors. Applied Sonochemistry. Wiley-VCH Verlag GmbH; Weinheim: 2002.

10). Zimm BH, Stockmayer WH. J. Chem. Phys 1949;17:1301–1314.

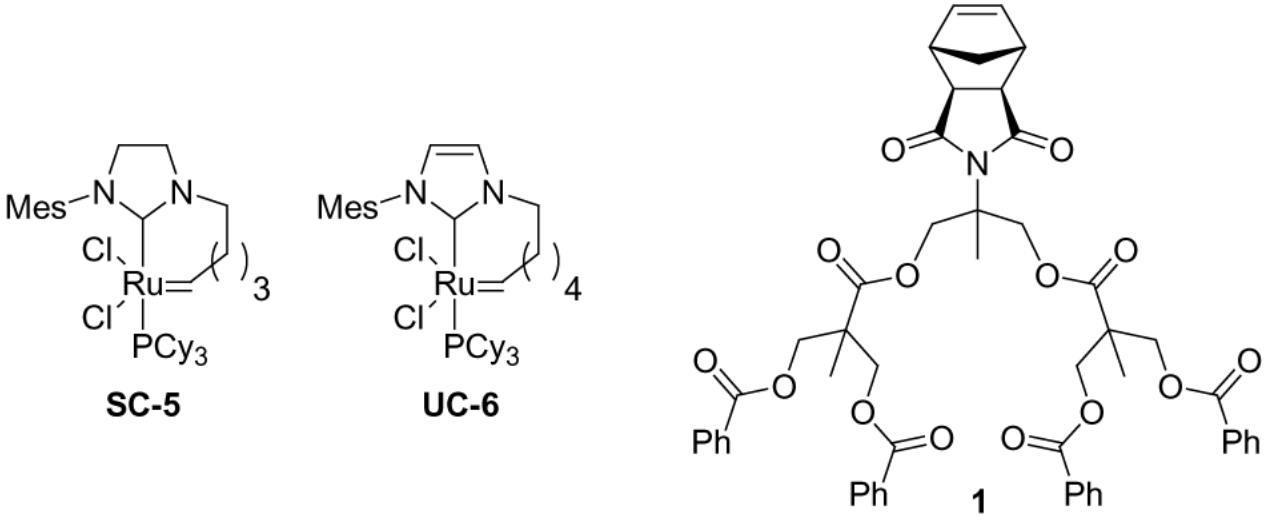

Figure 1.
Structures of the cyclic REMP catalysts and dendronized macromonomer used in this study.

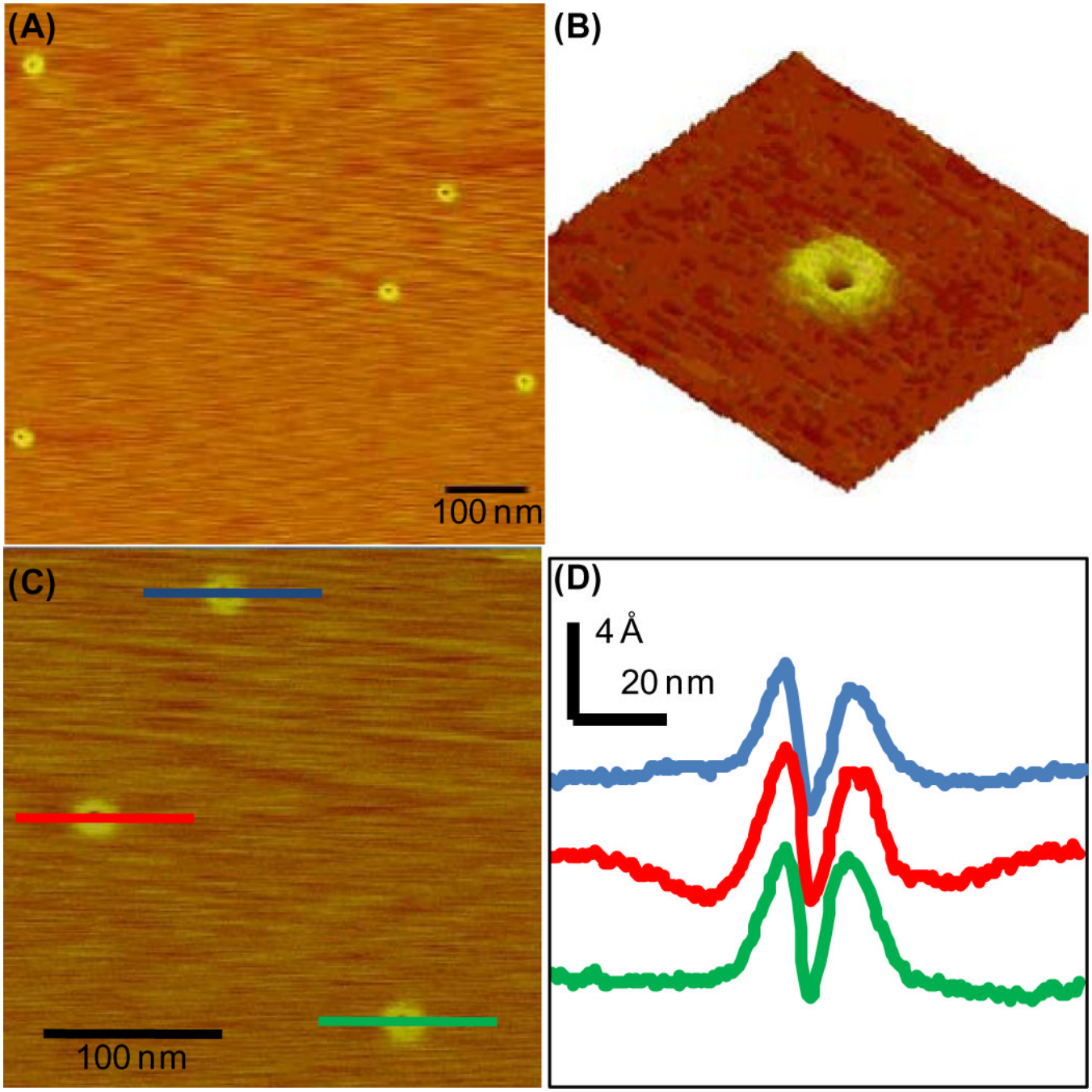

Figure 2.
(A) AFM images of **P1** (Table 1, entry 7) on mica. (B) 3-D plot of toroidal feature. (C) Three toroids from image (A). (D) Line scans of toroids in image (C).

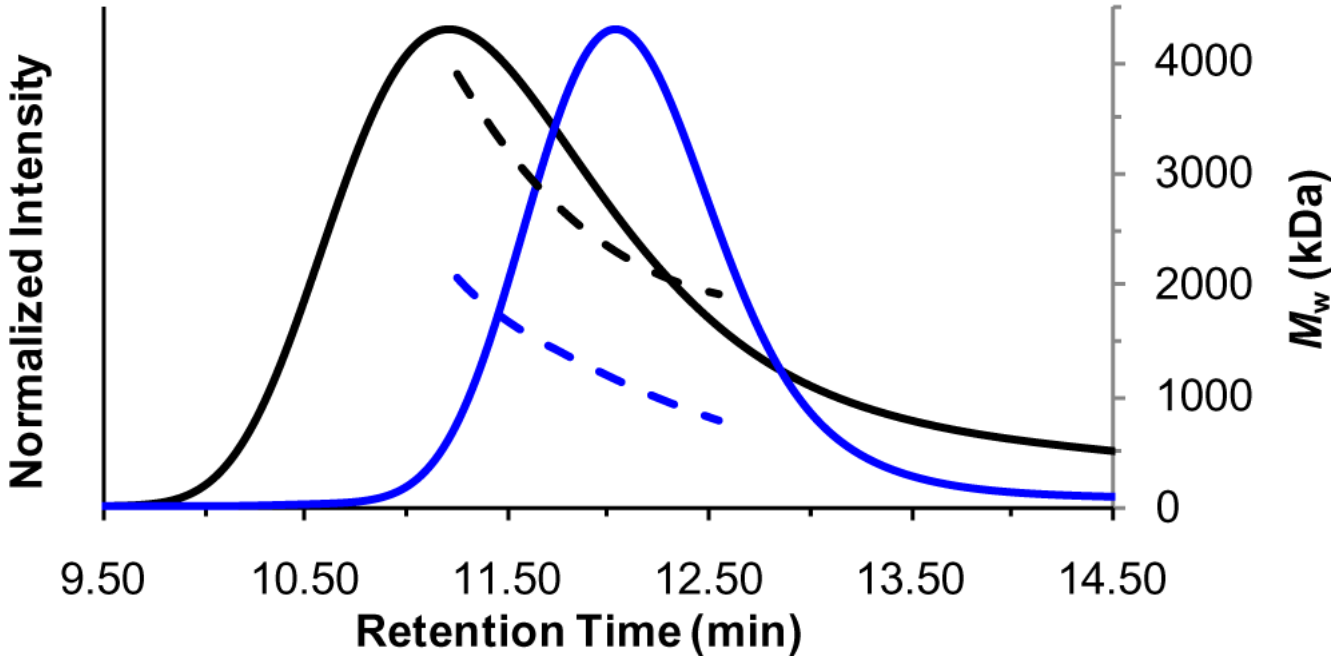

Figure 3.
GPC data for **P1** (black) and **P1$_{son}$** (blue): normalized refractive index detector intensities (solid lines) and M_w values (dashed lines) *vs* retention times.

Table 1

REMP of **1** to give cyclic dendeonized polymer **P1**[a].

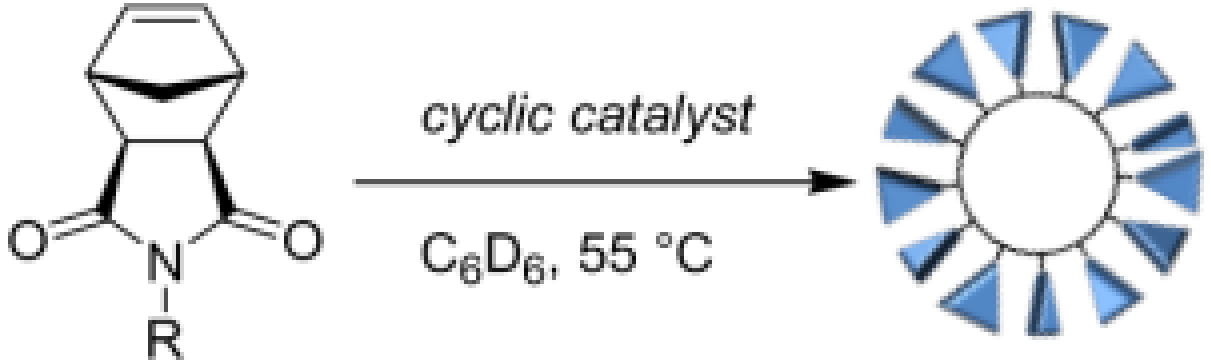

Entry	Catalyst	$[1]_0$(M)	$[1]_0/[C]_0$	M_w (MDa)[b]	DP/1000	PDI[b]
1	**SC-5**	0.05	50	5.26	5.84	1.29
2	**SC-5**	0.10	50	4.06	4.51	1.25
3[c]	**SC-5**	0.10	100	4.47	4.97	1.51
4[d]	**SC-5**	0.10	200	5.33	5.92	1.49
5	**SC-5**	0.20	50	3.90	4.33	1.33
6	**SC-5**	0.33	50	1.97	2.19	1.17
7	**UC-6**	0.10	250	3.79	4.21	1.18

[a] Unless noted otherwise, reactions were conducted under dry N_2 and monitored via ^{1}H NMR spectroscopy until conversions were >90%. $[\mathbf{1}]_0$ = initial concentration of **1**; $[\mathbf{C}]_0$ = initial catalyst concentration

[b] Molecular weight data obtained via GPC with multiangle laser light scattering.

[c] Maximum conversion = 60%.

[d] Maximum conversion = 39%